

The Influence of Phototrophic Biomass on Fe and S Redox Cycling in an Acid Mine Drainage-Impacted System

John M. Senko · Doug Bertel · Thomas J. Quick ·

William D. Burgos

Received: 19 April 2010/Accepted: 11 August 2010/Published online: 29 August 2010
© Springer-Verlag 2010

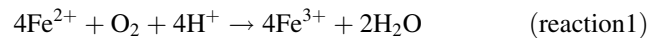
Abstract We examined the effects of organic carbon from oxygenic photosynthetic algal biomass on the redox cycling of Fe and S in an acid mine drainage (AMD)-impacted system. Fe(III)-rich sediments from the field site with abundant algae contained fewer Fe(II) oxidizing bacteria and lower rates of Fe(II) oxidation compared to sediments that did not contain abundant algae. The addition of algal biomass to sediments that did not previously contain abundant algae inhibited microbiological Fe(II) oxidation and enhanced microbiological Fe(III) and sulfate reduction. As Fe(III) reduction proceeded, sulfate was released into solution due to the reductive solubilization of Fe(III) (hydr)oxy-sulfate phases. Our results indicate that in systems where oxidative precipitation of Fe is exploited as an AMD treatment strategy, the abundant organic carbon provided by photosynthetic organisms may inhibit or reverse Fe(II) oxidation.

Keywords Acid mine drainage · Anaerobic processes · Phototrophic · Iron reduction · Sulfate reduction

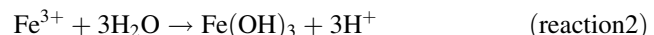
Introduction

One of the most pressing objectives of the treatment of acid mine drainage (AMD) is the removal of dissolved Fe

before the AMD enters waterways. An attractive approach to Fe removal is to exploit the activities of aerobic, acidophilic Fe(II) oxidizing bacteria (FeOB). We have previously observed such activities in a variety of AMD-impacted systems in which the AMD flows as a sheet (approximately 0.5–1 cm in depth) over the terrestrial surface (DeSa et al. 2010; Senko et al. 2008). The sheet-flow characteristics of these systems enhance the diffusion of O₂ into the AMD, thereby enhancing the activities of FeOB, which couple the oxidation of Fe(II) to the reduction of O₂:



In the pH range typically encountered in Appalachian coal mine-derived AMD (pH 2.5–4.5; Cravotta 2008), biogenic Fe(III) subsequently hydrolyzes and precipitates from solution:



These sheet-flow systems may be considerably more sustainable approaches to AMD treatment, since they would limit or eliminate high energy, material, and labor costs associated with other treatment schemes (Rose et al. 2004; Weaver et al. 2004). The shallow AMD depth provides efficient passive aeration of fluids and we have identified several sheet-flow systems in which Fe(II) is oxidatively precipitated from AMD with no human intervention to stimulate the process (DeSa et al. 2010; Senko et al. 2008).

Photosynthetic microeukaryotes, including green algae, euglenoids, and diatoms are commonly encountered in AMD systems, and their activities may produce O₂ concentrations as high as 21 mg/L (Brake et al. 2001a, b, 2004; Sanchez-España et al. 2007). From the perspective of stimulating oxidative precipitation of Fe from AMD, the

J. M. Senko (✉) · D. Bertel · T. J. Quick
Department of Geology and Environmental Science,
The University of Akron, Akron, OH 44325, USA
e-mail: senko@uakron.edu

W. D. Burgos
Department of Civil and Environmental Engineering,
The Pennsylvania State University, University Park,
PA 16802, USA

activities of these organisms may be considered beneficial since they provide more O₂ for FeOB than could be achieved by passive diffusion of atmospheric O₂ alone. However, photosynthetic activities also lead to the entrainment of organic carbon in AMD-impacted systems. Abundant organic carbon may inhibit the activities of FeOB (Johnson 1995, 1997; Marchand and Silverstein 2003) or enhance the activities of Fe(III) and sulfate reducing bacteria (FeRB and SRB, respectively), leading to the reductive re-release of dissolved Fe(II) or accumulation of sulfide-containing minerals within the sediments (Bridge and Johnson 2000; Fortin and Praharaj 2005; Herlihy and Mills 1985; Johnson and Hallberg 2002; Küsel and Dorsch 2000; Küsel et al. 1999, 2001; Peine et al. 2000; Senko et al. 2009). Indeed, algal biomass has been used to stimulate sulfate reduction in cases where stimulation of SRB activities is chosen as an AMD treatment strategy (Boshoff et al. 2004).

In light of the beneficial and detrimental outcomes of photosynthetic activity in AMD sheet-flow treatment systems, we compared the abundances of FeOB and rates of microbiological Fe(II) oxidation associated with photosynthetic algal mats and with algae-free sediments obtained from an coal mine-derived AMD-induced kill zone in southwestern Pennsylvania, USA. We also assessed the impact of phototrophic biomass on microbiological Fe and S redox cycling in these sediments.

Materials and Methods

Site Description

The Hughes Borehole AMD site is located in Cambria County, PA (40°24'32.46"N, 78°39'17.63"W). The borehole was installed in the 1920s to alleviate hydraulic pressure in an abandoned deep coal mine, but was subsequently capped. In the 1970s, the cap ruptured (Zink et al. 2005), leading to the flow of AMD at a rate of 800–3,500 gpm. Over the approximately 40 years since the cap rupture, the AMD has induced a “kill zone” of approximately 24,000 m². The sediments in the kill zone are composed primarily of Fe(III) (hydr)oxide precipitates that are a result of oxidation of Fe(II) in the AMD, and subsequent hydrolysis of Fe³⁺. Dissolved Fe of the emergent AMD at the Hughes Borehole is predominantly Fe(II), and the pH is 4.1 (Table 1).

AMD flows through and over the kill zone in two distinct flow regimes: (1) deep (approximately 250 mm) channels (referred to as channel-flow) and (2) as broad sheets of AMD spread over the kill zone with depths of approximately 5–10 mm (referred to as sheet-flow) (DeSa et al. 2010). During a sampling campaign in October, 2006, we collected sediments and AMD from channel-flow

Table 1 Temperature and dissolved constituents of emergent AMD at the Hughes Borehole site

Temperature	13°C
pH	4.1
D.O.	0.61 mg/L
Conductivity	1174 µS/cm
Sulfate	6.0 mM
Dissolved Fe(II)	1.9 mM
Dissolved Fe(III)	0.13 mM
Mg	1.3 mM
Ca	0.54 mM
Al	0.44 mM
Chloride	0.33 mM
Cu	0.31 mM
Na	0.2 mM
K	0.13 mM
Mn	0.015 mM

(referred to as B5) and sheet-flow paths (referred to as C5). Channel-flow regimes contained filamentous mats of green photosynthetic algae (Fig. 1b). Similar filamentous algal mats have been reported in AMD-impacted systems and have been classified as belonging to the phylum Chlorophyta (Sanchez-España et al. 2007). Algal mats in B5 were most abundant and massive (approximately 3 cm deep) from April to October, and were rarely observed in winter months. As a result of the seasonality of algal mat growth, we observed layering of mineral phases, where orange Fe(III) (hydr)oxide phases were underlain by a black iron-sulfide layer (Fig. 1a). The iron-sulfide layer contained voids, which appeared to be remnants of gas bubbles produced by the algae (Fig. 1a, b). These observations suggested that the seasonal death and subsequent burial of algal biomass by Fe(III) (hydr)oxide phases fueled sulfate reduction in deeper sediments. Sheet-flow regimes (C5) did not contain abundant algal mats, but rather appeared to be mostly composed of Fe(III) (hydr)oxide phases (Fig. 1c). The Fe(III) (hydr)oxide surfaces in C5 (i.e. sheet-flow) regions were not underlain by black iron-sulfide phases.

Field Sampling

Sediment samples were collected in the B5 and C5 regions of the Hughes Borehole AMD system. Samples from the Hughes Borehole and AMD-impacted systems in Washington and Indiana Counties, PA were collected with a sterile spatula, transferred to sterile mason jars or whirl-paks, and stored on ice for transport to the laboratory. AMD water samples for chemical analysis were filter sterilized in the field and stored on ice for transport to the laboratory. Samples for analysis of dissolved metals were acidified with 0.5 M HCl.

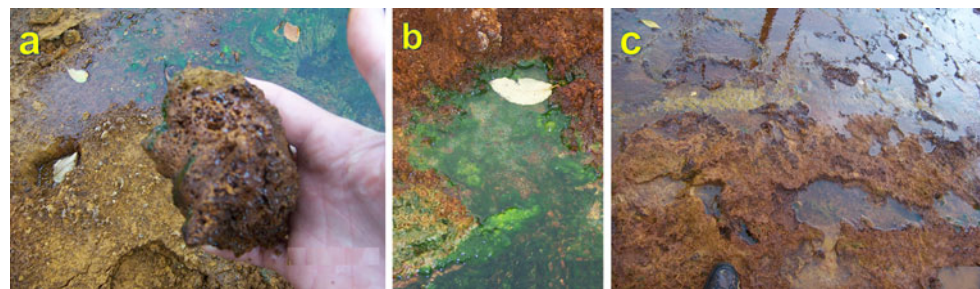


Fig. 1 Overview of sampling sites at the Hughes Borehole AMD site, including crusts associated with the B5 sampling point that indicate the presence of iron-sulfide phases (**a**), photosynthetic organisms at

the B5 sampling point (**b**), and the sheet-like flow characteristics of the C5 sampling point (**c**). Hand (panel **a**), and approximately 6 cm leaves (panels **b**, **c**) provide scale

FeOB Enumeration

FeOB were enumerated by plate counting technique using FeTSBo medium (Johnson 1995). Briefly, the medium contained FeSO_4 (25 mM), $(\text{NH}_4)_2\text{SO}_4$ (14 mM), MgSO_4 (2 mM), and trypticase soy broth (0.25 g/L), and the pH was adjusted to 3.5 with H_2SO_4 . Agarose (20 g/L) was used as a solidifying agent. An underlayer was inoculated (2.5% v/v) with *Acidiphilium organovorum*, allowed to solidify, and followed by an *A. organovorum*-free overlayer. The *A. organovorum*-inoculated underlayer was included to consume products of agarose hydrolysis that accumulate at low pH and may inhibit FeOB. Samples were serially diluted in Fe(II)- and agarose-free FeTSBo and spread on the plates. FeOB (as colony forming units; CFU) were indicated by the formation of orange-brown colonies.

Sediment Incubations

For experiments to determine rates of Fe(II) oxidation by algae-free and algae-containing flow regions of the Hughes Borehole system, sediments collected from the B5 and C5 sampling locations of the Hughes Borehole were incubated with filter-sterilized synthetic AMD (SAMD) that contained 5 mM FeSO_4 , 5 mM CaSO_4 , 4 mM MgSO_4 , 1 mM Na_2SO_4 , 0.5 mM $\text{Al}_2(\text{SO}_4)_3$, 0.4 mM MnSO_4 , and 0.1 mM $(\text{NH}_4)_2\text{Fe}(\text{SO}_4)_2$. The pH was adjusted to 3.5 with H_2SO_4 and the SAMD was amended with a filter-sterilized solution of FeSO_4 to achieve a Fe(II) concentration of 5 mM (Senko et al. 2008). Sediments (8 g) were incubated with 25 ml of SAMD in sealed 160 ml serum bottles with air in the headspace. Formaldehyde (1%) was added to deactivate microbiological activity in negative controls. Sediment incubations were conducted in the dark, and samples were periodically removed using a needle and syringe, the pH of sediment-SAMD suspensions was measured, and dissolved Fe(II) was quantified as described below. First order Fe(II) oxidation rate constants (k , time $^{-1}$) were determined by

linear least squares regression fitting of $\ln[\text{Fe(II)}]$ versus time using the following equation:

$$\ln[\text{Fe(II)}_t] = -kt + \ln[\text{Fe(II)}_{\text{initial}}] \quad (1)$$

For experiments to assess the effect of algal biomass on rates of Fe(II) oxidation by microbial communities associated with sediments that did not initially contain algal biomass (C5), algal mats were collected from the B5 region of the Hughes Borehole system, washed three times with Fe(II)-free SAMD, and resuspended in SAMD. Suspensions were subsequently homogenized in a blender and oxygen was removed from the suspensions by bubbling under a stream of sterile N_2 . Suspensions were autoclaved and provided to sediment incubations containing 10 g C5 sediment, 50 mL SAMD, and 10 mM FeSO_4 to achieve organic carbon concentrations of 0 (no biomass amendment), 0.1, 0.5, and 1 g/L. Microbiological activity was deactivated in negative controls using 1% formaldehyde. Incubations contained air in the headspace, and after incubations had proceeded for 55 days, the headspace of selected bottles was replaced with additional filter-sterilized air. Samples were periodically removed using a needle and syringe in an anoxic glovebag (Coy Laboratory Products Inc., Grass Lake, MI, USA), and pH, sulfate, sulfide, and Fe(II) were quantified as described below.

Analytical Techniques and Sediment Incubation Sampling

Field temperature, pH, D.O., and conductivity were measured using portable meters. Dissolved Fe(II) in field samples was measured using the 1,10-phenanthroline assay (Tamura et al. 1974). To quantify dissolved Fe(III), field samples were incubated in an anoxic glovebag for approximately 24 h with 0.25 hydroxylamine-HCl/0.25 M HCl, which reduced Fe(III) to Fe(II), and Fe(II) was subsequently quantified using the 1,10-phenanthroline assay. Dissolved Al, Ca, K, Mg, Mn, and Na were quantified in 0.5 M HCl-acidified samples by inductively coupled

plasma emission spectrometry using a Leeman Labs PS3000UV ICP-AES system (Teledyne Leeman Labs, Hudson, NH, USA). Sulfate and chloride were quantified by ion chromatography using a Dionex 100 system with an AS4A column and conductivity detector (Dionex Corp., Sunnyvale, CA, USA). Total organic carbon in the algal suspension was determined using a Shimadzu total organic carbon analyzer TOC-Vcsn (Shimadzu Corp., Columbia, MD, USA).

The pH of sediment incubations was taken directly from subsamples of sediment-SAMD suspensions using a Thermo-Orion PerpHecT semi-micro combination pH electrode and 550A pH meter (ThermoFisher Scientific, Waltham, MA, USA). To measure sulfate and soluble Fe(II) in sediment incubations, sediments were separated from the soluble fraction by centrifugation. The supernatant was removed and sulfate was measured by ion chromatography (described above). Soluble Fe(II) was preserved in 0.5 M HCl, and quantified by ferrozine assay (Lovley and Phillips 1987). To measure solid phase Fe(II) (e.g. precipitated with sulfide or adsorbed to mineral phases), sediment-SAMD suspensions were incubated in 0.5 M HCl for approximately 16 h, and remaining sediments were separated from the soluble fraction by centrifugation. Fe(II) in the supernatant was quantified by ferrozine assay, and insoluble Fe(II) was calculated by the difference between 0.5 M HCl-extractable Fe(II) and soluble Fe(II) (Lovley and Phillips 1987). Samples for sulfide analysis, including suspensions of SAMD and sediment (and associated FeS phases, if present), were preserved in 10% zinc acetate, and sulfide was quantified by methylene blue assay (Cline 1969). Powder X-ray diffraction (XRD) was conducted using a Phillips PW 1710 automated diffractometer system.

Results and Discussion

Abundances of FeOB and Rates of Fe(II) Oxidation

We compared the abundance of FeOB associated with algae-containing (B5) and algae-free (C5) sediment samples. FeOB were more abundant in C5 sediments than in B5 sediments (Table 2). When B5 and C5 sediments were incubated under oxic conditions and in the absence of light, Fe(II) oxidation proceeded at a greater rate in the C5 sediments compared to B5 sediments (Fig. 2, Table 2). In previous incubations using sediments from another AMD-impacted system, we did not observe accumulation of dissolved Fe(III), suggesting that when Fe(II) is oxidized to Fe(III) (reaction 1), it rapidly hydrolyzes and precipitates as Fe(III) (hydr)oxide phases (reaction 2) (Senko et al. 2008). Sediments with lower numbers of FeOB (B5)

Table 2 Abundance of Fe(II) oxidizing bacteria and first order rate constants of Fe(II) oxidation (k) and in incubations containing B5 or C5 sediments

	Fe(II) oxidizing bacteria (CFU/g sediment)	Fe(II) oxidation k (day $^{-1}$)
B5 sediments	$9.5 \times 10^3 \pm 4.4 \times 10^2$	3.5
C5 sediments	$1.6 \times 10^5 \pm 7.2 \times 10^4$	5.3

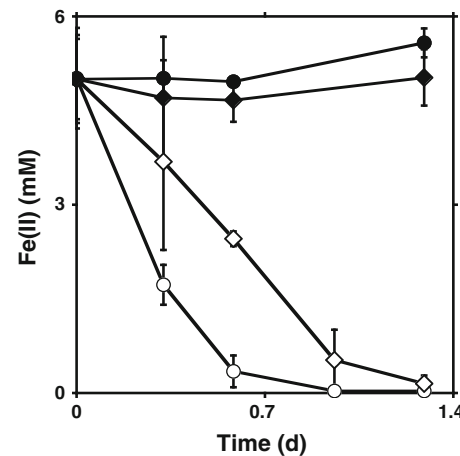


Fig. 2 Fe(II) oxidation in incubations containing non-sterile (open diamond) or biologically deactivated (filled diamond) B5 sediments and non-sterile (open circle) or biologically deactivated (filled circle) C5 sediments from the Hughes Borehole AMD site

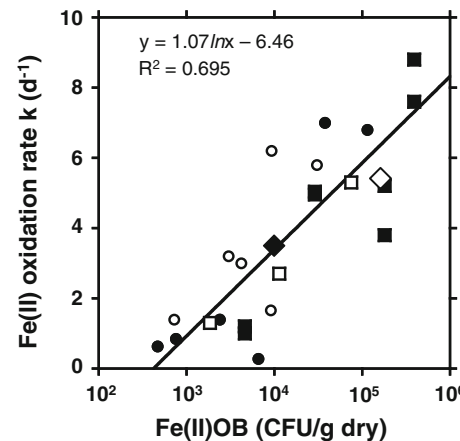


Fig. 3 Relationship between abundance of Fe(II) oxidizing bacteria (FeOB) and first order rate constants (k) of Fe(II) oxidation in AMD-impacted systems from McKean County (open circle), Clearfield County (filled circle), Washington County (open square), and Indiana County (filled square), Pennsylvania, and the B5 (filled diamond) and C5 (open diamond) sampling points of the Hughes Borehole site. Values from the McKean County and Clearfield County sampling sites are from Senko et al. (2008)

exhibited lower rates of Fe(II) oxidation, while sediments with higher numbers of FeOB (C5) exhibited higher rates of Fe(II) oxidation (Table 2). Indeed, the first-order rate

constants and FeOB abundances observed in both the B5 and C5 sediments fall within the correlation between Fe(II) oxidation rate and FeOB abundances that we have observed in several AMD-impacted systems (Fig. 3). Therefore, abundance of FeOB may be a useful predictor of the efficiency of oxidative precipitation in systems designed to oxidatively precipitate Fe(II) from AMD (DeSa 2010; Kirby et al. 1999; Nengovhela et al. 2004; Senko et al. 2008). These observations suggest that algal organic matter inhibits the activities and perhaps growth of FeOB in the Hughes Borehole system. The algal organic carbon may enhance organotrophic microbial activities and diminish the availability of O₂, which is required for efficient FeOB activity (Senko et al. 2008). Alternatively, algal organic carbon may be toxic to FeOB, thus directly inhibiting their activities (Johnson 1995; Marchand and Silverstein 2003).

Effects of Algal Organic Carbon on Fe and S Cycling

To assess the effects of algal biomass on Fe(II) oxidation by microorganisms associated with C5 sediments (i.e. sediments that exhibited relatively high rates of Fe(II) oxidation in previous experiments), we incubated these sediments with 0, 0.1, 0.5, and 1 g/L algal organic carbon (OC). Few chemical changes were observed in formaldehyde-deactivated controls (Figs. 4, 5). The pH of formaldehyde-deactivated incubations decreased, likely due to acidity associated with Fe(III) phases. For instance, Petyazhko et al. (2009) have suggested that Fe(III) phases (e.g. schwertmannite) in AMD-impacted systems may exert considerable control on the pH of fluids, regardless of the initial chemical composition of those fluids. These results suggest that the chemical changes that we observed in non-sterile incubations were attributable to

Fig. 4 Dissolved Fe(II) (panels **a**, **b**), solid phase Fe(II) (panels **c**, **d**), sulfate (panels **e**, **f**), sulfide (panels **g**, **h**) concentrations, and pH (panels **i**, **j**) in C5 sediments amended with 0 or 0.1 g/L photosynthetically-derived organic carbon in non-sterile (filled circle) and biologically deactivated (open circle) incubations. Dashed lines represent the time at which the headspaces of selected serum bottles were re-amended with air. Respective analytes in air re-amended bottles are represented by open square. Note differences in scale of dissolved Fe(II) in panels (**a**) and (**b**). Data depicted in Fig. 4 are from experiments run concurrently with the experiments shown in Fig. 5. Note differences in scale of panels **a–h** of Figs. 4 and 5

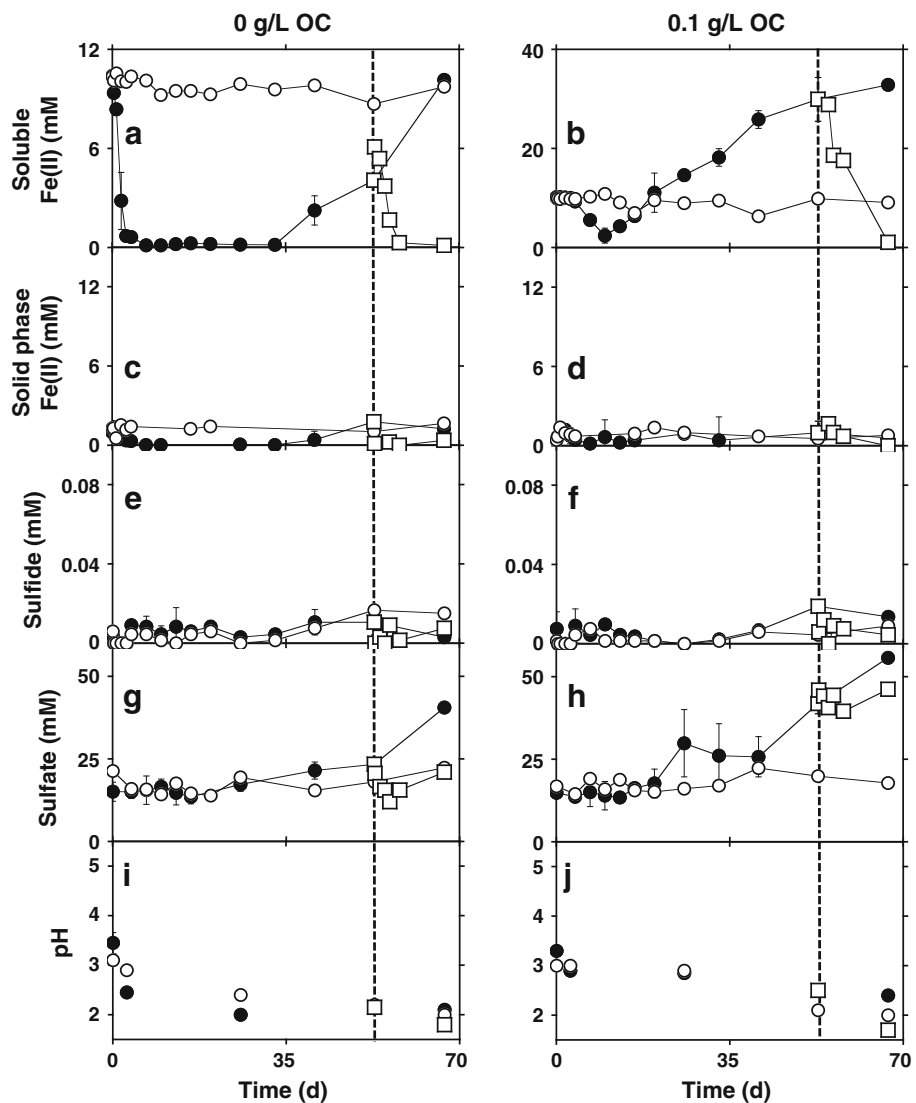
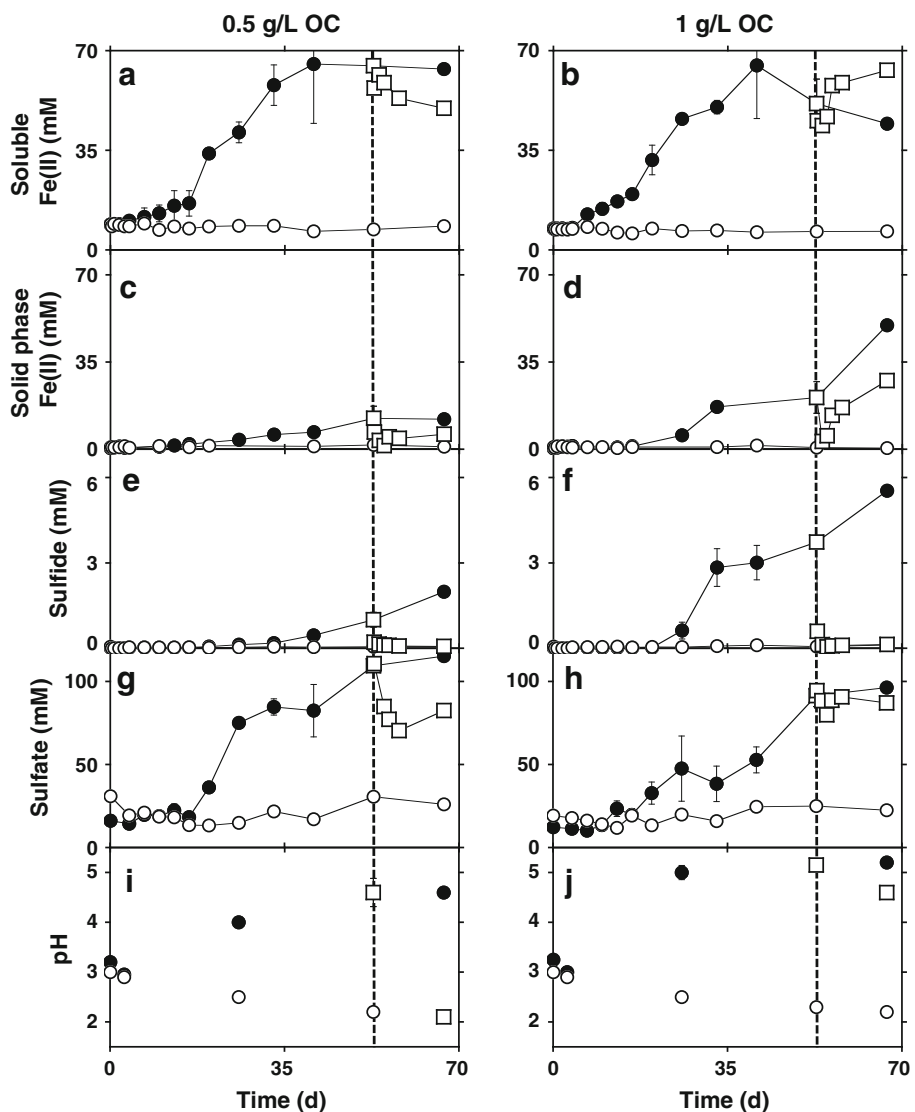


Fig. 5 Dissolved Fe(II) (panels **a**, **b**), solid phase Fe(II) (panels **c**, **d**), sulfate (panels **e**, **f**), sulfide (panels **g**, **h**) concentrations, and pH (panels **i**, **j**) in C5 sediments amended with 0.5 or 1 g/L photosynthetically-derived organic carbon in non-sterile (*filled circle*) and biologically deactivated (*open circle*) incubations. *Dashed lines* represent the time at which the headspaces of selected serum bottles were re-amended with air. Respective analytes in air re-amended bottles are represented by *open square*. Data depicted in Fig. 5 are from experiments run concurrently with the experiments shown in Fig. 4. Note differences in scale of panels (**a**–**h**) of Figs. 4 and 5

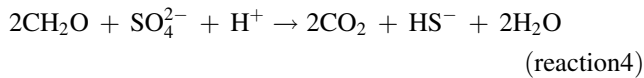
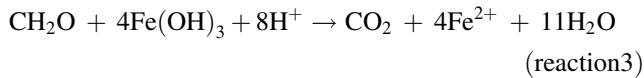


microbiological activity. In algal OC-free incubations (0 g/L), soluble Fe(II) was rapidly oxidized and precipitated and accompanied by a decrease in pH (Fig. 4a, i), indicating the hydrolysis and precipitation of biogenic Fe^{3+} (reaction 2). Throughout these experiments, solid phase Fe(II) comprised a relatively small fraction of the total Fe(II) (Fig. 4c). After the initial oxidative precipitation of Fe, Fe(II) concentrations remained low until approximately 35 days of incubation, after which we observed the re-release of Fe(II) (Fig. 4a, i), likely due to complete consumption of O_2 and onset of Fe(III) reducing conditions. No sulfidogenesis was observed in these incubations, but sulfate concentration increased as Fe(III) reduction proceeded (Fig. 4g).

In incubations amended with 0.1 g/L algal OC, Fe(II) oxidation was delayed, and oxidative precipitation was incomplete (Fig. 4b). Upon cessation of Fe(II) oxidizing activity, Fe(III) reduction began, with dissolved Fe(II)

accumulating to 30 mM after approximately 55 days, and a concurrent increase in sulfate concentration (Fig. 4b, h). Little solid phase Fe(II) was detected in these incubations, since the pH remained at approximately 3.0 throughout the incubations, which enhanced the solubility of Fe(II) (Fig. 4d, j). Addition of 0.5 and 1 g/L algal OC completely inhibited Fe(II) oxidation, and Fe(III) reduction commenced within 5 days of initiation of the experiments (Fig. 5a, b). Sulfidogenesis was observed in these incubations after 35 days (Fig. 5e, f). An increase in solid phase Fe(II) (Fig. 5c, d) occurred concurrently with pH increase (Fig. 5i, j) in these incubations. Higher pH enhanced adsorption of Fe(II) to remnant solid phases, since Fe(II) sorption was minimal in biologically-deactivated controls where no pH increase occurred (Fig. 5i, j). As sulfate reduction proceeded, a fraction of solid phase Fe(II) was likely attributable to the formation of iron-sulfide phases. Anaerobic activities lead to an increase in pH of AMD-

impacted systems via reduction of Fe(III) (hydr)oxides ([reaction 3](#)), conversion of strongly acidic sulfate to weakly acidic sulfide ([reaction 4](#)), and production of carbonate alkalinity ([reaction 3](#) and [reaction 4](#)) (Fortin and Praharaj [2005](#); Piene et al. [2000](#); Senko et al. [2009](#)).



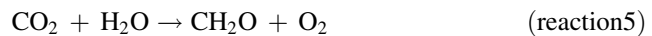
It is notable that dissolved sulfate accumulated (Figs. [4g](#), [h](#), [5g](#), [h](#)) in all incubations concurrently with Fe(III) reduction (Figs. [4a](#), [b](#), [5a](#), [b](#)), despite evidence of sulfate reduction (i.e. sulfidogenesis) in incubations amended with 0.5 and 1 g/L algal OC (Fig. [5e](#), [f](#)). This release of sulfate may be due to the reductive solubilization of sulfate-containing Fe(III) phases. Schwertmannite ($\text{Fe}_8\text{O}_8(\text{OH})_{8-2x}(\text{SO}_4)_x\text{nH}_2\text{O}$, where $1 \leq x \leq 1.5$) is sulfate-containing Fe(III) phase that is frequently encountered in AMD-impacted systems (DeSa et al. [2010](#); Murad and Rojík [2005](#); Peretyazhko et al. [2009](#); Regenspurg et al. [2004](#); Schwertmann et al. [1995](#)). Such minerals form in acidic, sulfate-rich fluids when sulfate ions are incorporated into the mineral structure (Bigham et al. [1990](#), [1996](#); Gagliano et al. [2004](#); Murad and Rojík [2005](#)). Indeed, XRD analysis of Fe(III) phases recovered from the C5 sampling region of the Hughes Borehole revealed the presence of schwertmannite (Fig. [6](#)). Given the stoichiometry of Fe(III) and sulfate in schwertmannite, we would expect a release of 1–1.5 mol sulfate for every 8 mol Fe(II) produced via reduction of schwertmannite-Fe(III). However we have observed a sulfate:Fe(II) ratio of approximately 1:1 (e.g. Fig. [5b](#), [d](#),

[h](#)). The discrepancy may be due to the release of sulfate adsorbed to Fe(III) phases, but not necessarily incorporated in the mineral matrix (Küsel and Dorsch [2000](#); Peretazhko et al. [2009](#)).

We hypothesized that the inhibition of Fe(II) oxidizing activity and enhancement of anaerobic processes (i.e. Fe(III) and sulfate reduction) that we observed were due to depletion of O_2 in the sediment incubations, and that algal biomass enhanced the depletion of O_2 . After 55 days of incubation, the headspace of selected incubations was replaced with filter-sterilized air to provide additional O_2 . Upon addition of O_2 to algal organic carbon-unamended incubations and incubations amended with 0.1 g/L algal OC, Fe(II) that had been produced via Fe(III) reduction was rapidly oxidized, and sulfate release halted (Fig. [4a](#), [b](#), [g](#), [h](#)). The addition of O_2 to incubations amended with 0.5 g/L algal OC led to the oxidation of approximately 15 mM Fe(II) and rapid sulfide oxidation (Fig. [5a](#), [e](#)). The decrease in pH and sulfate concentration in these incubations (Fig. [5g](#), [i](#)) suggests the coprecipitation of Fe(III) and sulfate to form Fe(III) (hydr)oxy-sulfate phases. In incubations amended with 1 g/L algal OC, we observed a temporary cessation of Fe(III) reduction, which returned to previous rates after 2 days (Fig. [4b](#), [d](#)), suggesting that sufficient organic carbon remained in these incubations to drive the rapid consumption of O_2 , after which anaerobic processes resumed. The resumption of Fe(II) oxidation upon reamendment with O_2 in incubations amended with 0.1 or 0.5 g/L OC suggests that algal OC served as a competitive electron donor with Fe(II) and led to the consumption of O_2 , thus stimulating anaerobic processes (i.e. Fe(III) and sulfate-reduction).

Environmental Implications

Due to the relatively harsh chemical conditions (i.e. low pH, high dissolved solids) of AMD-impacted systems, phototrophic microeukaryotes may be the only photosynthetic organisms capable of surviving in such systems (Brake et al. [2001a](#), [2004](#); Rowe et al. [2007](#)). As such, these organisms may represent the primary sources or organic carbon in AMD-impacted systems (Rowe et al. [2007](#)). Based on the stoichiometry of oxygenic photosynthesis ([reaction 5](#)), for every mole of oxygen produced, one mole of organic carbon should be left behind in these systems.



Since much of this oxygen is likely to be degassed from the AMD, organic carbon represents the primary geochemical legacy of photosynthetic microeukaryotes. While oxygenic photosynthetic organisms may temporarily enhance oxidation of Fe(II) (Brake et al. [2001a](#), [2002](#)), the entrainment of organic carbon via their activities may

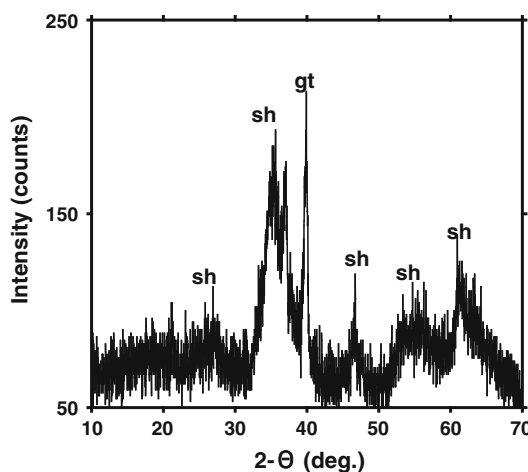


Fig. 6 X-ray powder diffraction of Fe(III) sediments collected from the C5 sampling point of the Hughes Borehole; “sh” denotes peaks corresponding to schwertmannite, “gt” denotes peaks corresponding to goethite

ultimately lead to the “futile cycling” of Fe and S (Johnson and Hallberg 2002), in which any enhancement of Fe(II) oxidation achieved by greater oxygen availability may be reversed due to the abundant organic carbon produced by oxygenic photosynthetic organisms. Our results suggest that FeOB are less abundant in AMD systems with abundant algae. The presence of photosynthetic microeukaryotic biomass inhibits the activities of FeOB and enhances anaerobic processes, which are detrimental to the overall goal of oxidative precipitation of Fe from AMD. As such, prevention of photosynthetic primary productivity may be an important design consideration if sheet-flow systems are implemented as an AMD treatment strategy. Exclusion of sunlight from the sheet-flow systems is a potential strategy for preventing the proliferation of algae, but this may prove to be impractical. Our experience at the Hughes Borehole system suggests that algae proliferate in channelized (e.g. B5) regions of the system, but not when AMD flows as a 5 mm-deep sheet (e.g. C5). Maintenance of sheet-flow conditions may be a simple means of both enhancing aeration of AMD and minimizing photosynthetic algal organic carbon inputs.

Acknowledgments We thank Malcolm Crittenden for providing samples from Indiana County, Pennsylvania. This work was supported by the Pennsylvania Dept of Environmental Protection, Bureau of Abandoned Mine Reclamation, the Pennsylvania Water Resources Research Center at The Pennsylvania State University, and a faculty research grant provided by the University of Akron.

References

- Bigham JM, Schwertmann U, Carlson L, Murad E (1990) A poorly crystallized oxyhydroxysulfate of iron formed by bacterial oxidation of Fe(II) in acid mine waters. *Geochim Cosmochim Acta* 54:2743–2758
- Bigham JM, Schwertmann U, Traina SJ, Winland RL, Wolf M (1996) Schwertmannite and the chemical modeling of iron in acid sulfate waters. *Geochim Cosmochim Acta* 60:2111–2121
- Boshoff G, Duncan J, Rose PD (2004) The use of micro-algal biomass as a carbon source for biological sulfate reducing systems. *Wat Res* 38:2659–2666
- Brake SS, Dannelly HK, Connors KA (2001a) Controls on the nature and distribution of an alga in coal mine-waste environments and its potential impact on water quality. *Environ Geol* 40:458–468
- Brake SS, Dannelly HK, Connors KA, Hasiotis ST (2001b) Influence of water chemistry on the distribution of an acidophilic protozoan in an acid mine drainage system at the abandoned Green Valley coal mine, Indiana, USA. *Appl Geochem* 16: 1641–1652
- Brake SS, Hasiotis ST, Dannelly HK, Connors KA (2002) Eukaryotic stromatolite builders in acid mine drainage: implications for precambrian iron formations and oxygenation of the atmosphere? *Geology* 30:599–602
- Brake SS, Hasiotis ST, Dannelly HK (2004) Diatoms in acid mine drainage and their role in the formation of iron-rich stromatolites. *Geomicrobiol J* 21:331–340
- Bridge TA, Johnson DB (2000) Reductive dissolution of ferric iron minerals by *Acidiphilum* SJH. *Geomicrobiol J* 17:193–206
- Cline JD (1969) Spectrophotometric determination of hydrogen sulfide in natural waters. *Limnol Oceanogr* 14:454–458
- Cravotta CA III (2008) Dissolved metals and associated constituents in abandoned coal-mine discharges, Pennsylvania, USA. Part 1: constituent quantities and correlations. *Appl Geochem* 23:166–202
- DeSa TC, Brown JF, Burgos WD (2010) Laboratory and field-scale evaluation of low-pH Fe(II) oxidation at the Huges Borehole, Portage, Pennsylvania. *Mine Water Environ* (in press)
- Fortin D, Praharaj T (2005) Role of microbial activity in Fe and S cycling in sub-oxic to anoxic sulfide-rich mine tailings: a mini-review. *J Nucl Radiochem Sci* 6:39–42
- Gagliano WB, Brill MR, Bigham JM, Jones FS, Traina SJ (2004) Chemistry and mineralogy of ochreous sediments in a constructed mine drainage wetland. *Geochim Cosmochim Acta* 68:2119–2128
- Herlihy AT, Mills AL (1985) Sulfate reduction in freshwater sediments receiving acid mine drainage. *Appl Environ Microbiol* 49:179–186
- Johnson DB (1995) Selective solid media for isolating and enumerating acidophilic bacteria. *J Microbiol Meth* 23:205–218
- Johnson DB (1997) Heterotrophic acidophiles and their roles in the bioleaching of sulfide ores. In: Rawlings DE (ed) Biomining: theory, microbes, and industrial processes. Springer, New York City, NY, USA, pp 259–280
- Johnson DB, Hallberg KB (2002) Pitfalls of passive mine water treatment. *Re/Views Environ Sci Bio/Technol* 1:335–343
- Kirby CS, Thomas HM, Southam G, Donald R (1999) Relative contributions of abiotic and biological factors in Fe(II) oxidation in mine drainage. *Appl Geochem* 14:511–530
- Küsel K, Dorsch T (2000) Effect of supplemental electron donors on the microbial reduction of Fe(III), sulfate, and CO₂ in coal mining-impacted freshwater lake sediments. *Microbial Ecol* 40:238–249
- Küsel K, Dorsch T, Acker G, Stackenbrandt E (1999) Microbial reduction of Fe(III) in acidic sediments: isolation of Acidiphilum cryptum JF-5 capable of coupling reduction of Fe(III) to oxidation of glucose. *Appl Environ Microbiol* 65:3633–3640
- Küsel K, Roth U, Trinkwalter T, Peiffer S (2001) Effect of pH on the anaerobic microbial cycling of sulfur in mining-impacted freshwater lake sediments. *Environ Experiment Bot* 46:213–223
- Lovley DR, Phillips EJP (1987) Rapid assay for microbially reducible ferric iron in aquatic sediments. *Appl Environ Microbiol* 53:1536–1540
- Marchand EA, Silverstein J (2003) The role of enhanced heterotrophic bacterial growth on iron oxidation by Acidithiobacillus ferrooxidans. *Geomicrobiol J* 20:231–244
- Murad E, Rojík P (2005) Iron mineralogy of mine-drainage precipitates as environmental indicators: review of current concepts and a case study from the Sokolov Basin, Czech Republic. *Clay Miner* 40:427–440
- Nengovhela NR, Strydom CA, Maree JP, Greben HA (2004) Chemical and biological oxidation of iron in acid mine water. *Mine Water Environ* 23:76–80
- Peretyazhko T, Zachara JM, Boily J-F, Xia Y, Gassman PL, Arey BW, Burgos WD (2009) Mineralogical transformations controlling acid mine drainage chemistry. *Chem Geol* 262:169–178
- Piene A, Tritschler A, Küsel K, Peiffer S (2000) Electron flow in an iron-rich acidic sediment—evidence for an acidity-driven iron cycle. *Limnol Oceanogr* 45:1077–1087
- Regenspurg S, Brand A, Peiffer S (2004) Formation and stability of schwertmannite in acidic mining lakes. *Geochim Cosmochim Acta* 68:1185–1197

- Rose AW, Biskom D, Daniel A, Bower MA (2004) An ‘autopsy’ of the failed Tangascootak #1 vertical flow pond. Proceedings of the national meeting of the American society of mining and reclamation, morgantown, WV, USA (CD)
- Rowe OF, Sánchez-España J, Hallberg KB, Johnson DB (2007) Microbial communities and geochemical dynamics in an extremely acidic, metal-rich stream at an abandoned sulfide mine (Huelva, Spain) underpinned by two functional primary production systems. *Environ Microbiol* 9:1761–1771
- Sanchez-España J, Pastor ES, Pamo EL (2007) Iron terraces in acid mine drainage systems: a discussion about the organic and inorganic factors involved in their formation through observations from the Tintillo acidic river (Riotinto mine, Huelva, Spain). *Geosphere* 3:133–151
- Schwertmann U, Bigham JM, Murad E (1995) The first occurrence of schwertmannite in a natural stream environment. *Eur J Mineral* 7:547–552
- Senko JM, Wanjugi P, Lucas M, Bruns MA, Burgos WD (2008) Characterization of Fe(II) oxidizing activities and communities at two acidic appalachian coalmine drainage-impacted sites. *ISME J* 2:1134–1145
- Senko JM, Zhang G, McDonough JT, Bruns MA, Burgos WD (2009) Metal reduction at low pH by a desulfosporosinus species: implications for the biological treatment of acidic mine drainage. *Geomicrobiol J* 26:71–82
- Tamura H, Goto K, Yotsuyanagi T, Nagayama M (1974) Spectrophotometric determination of iron(II) with 1, 10-phenanthroline in the presence of large amounts of iron(III). *Talanta* 21:314–318
- Weaver KR, Lagnese KM, Hedin RS (2004) Technology and design advances in passive treatment system flushing. Proceedings of the national meeting of the American society of mining and reclamation, morgantown, WV, USA (CD)
- Zink T, Wolfe A, Curley K (2005) Restoring the wealth of the mountains: cleaning up Appalachia’s abandoned mines. Trout Unlimited. <http://www.tu.org/atf/cf/%BED0023C4-EA23-4396-9371-8509DC5B4953%7D/TU%20AMD%20report.pdf>. Accessed 2 Apr 2010